electronics

MDPI

Article

Research on the Quantitative Assessment Method of HVDC Transmission Line Failure Risk during Wildfire Disaster

Bo Zhou *, Xinwei Sun, Yunyang Xu and Wei Wei

State Grid Sichuan Electric Power Research Institute, Chengdu 610041, China; sunxw09@126.com (X.S.); xuyunyang0912@163.com (Y.X.); weiwei0825sgcc@163.com (W.W.)
* Correspondence: zbv_s163@163.com

Abstract: It is increasingly important to effectively predict the failure of HVDC transmission lines caused by wildfire disasters. On the basis of comprehensively considering the distribution of fire points, the characteristics of wildfire propagation, and the failure factors of the transmission line, a method for calculating the probability of failure in HVDC transmission lines during wildfire disasters is proposed to quantify the risk of HVDC transmission line failures caused by wildfire disasters. Using the ArcGIS 10.7. platform, the study examined the quantity of fire points within the buffer zone of each HVDC transmission line from 2001 to 2022. The results indicate significant variations in the number of fire incidents in the buffer zones of various transmission lines. Notably, there has been a noticeable increase in the number of fire incidents along several HVDC transmission lines, including Xizhe, Baihetan-Jiangsu, Baihetan-Zhejiang, and Fufeng, in recent years. Based on the number of fire points in the buffer zone obtained through ArcGIS processing and the proposed failure probability calculation model, six HVDC hydropower transmission channels in the Sichuan Province were analyzed. At the same time, the proposed probability calculation model was simplified, and a corresponding linear evaluation index was introduced. The regression analysis results indicate that the proposed index can effectively assess the failure risk of HVDC transmission lines during wildfire disasters.

Keywords: risk assessment; HVDC transmission line; wildfire disasters; regression analysis

check for updates

Citation: Zhou, B.; Sun, X.; Xu, Y.; Wei, W. Research on the Quantitative Assessment Method of HVDC Transmission Line Failure Risk during Wildfire Disaster. *Electronics* **2024**, *13*, 2119. https://doi.org/10.3390/electronics13112119

Academic Editor: Ahmed Abu-Siada

Received: 1 May 2024
Revised: 25 May 2024
Accepted: 27 May 2024
Published: 29 May 2024

Copyright: © 2024 by the authors. Licensee MDPI, Basel, Switzerland. This article is an open access article distributed under the terms and conditions of the Creative Commons Attribution (CC BY) license (https://creativecommons.org/licenses/by/4.0/).

1. Introduction

The increasingly recurrent occurrences of wildfire disasters have caused significant damage to the earth's ecosystems in recent years. Simultaneously, the wildfire disasters have a significant impact on large-scale power transmission systems [1]. In 2018, numerous transmission lines in California were impacted by wildfire disasters, resulting in 87 fatalities, the destruction of approximately 2 million acres of land, and an economic loss of $16.5 billion [2]. As can be seen from the above case, the adverse effects of power system accidents caused by wildfire disasters are extremely serious. Due to the imbalance of energy distribution and the economic development level in China, HVDC transmission lines need to pass through densely vegetated mountainous areas. Wildfires caused by natural or man-made conditions are threatening the insulation safety and operational stability of HVDC transmission lines. According to statistics, the main HVDC transmission line tripping faults caused by wildfires in some provinces and regions account for 16% of the total number of faults and show an increasing trend [3]. Therefore, how to accurately calculate and rapidly assess the failure probability of transmission lines during wildfire disasters has become an extremely urgent problem.

From the occurrence of wildfire disasters to the failure of a wildfire-induced HVDC transmission line, the process can be divided into two stages. The spread of wildfire disasters and the subsequent burning process lead to a decrease in air gap insulation levels, resulting in the failure of HVDC transmission lines [4]. The above two processes are complex, and utilizing the two processes to calculate the failure probabilities of transmission

lines during wildfire disasters is an unrealistic thing. Experts and scholars have conducted related research work to simplify the calculating process of transmission line failure probability. In order to improve the stability of transmission lines, it is necessary to increase the monitoring of wildfire disasters. The main methods include wildfire prediction and early warning of wildfire spread [5,6].

2. Literature Review

For the wildfire diffusion process, Anderson et al. simplified the complex physical equations of the wildfire diffusion model and proposed a practical and simplified wildfire elliptical fire diffusion model [7]. Based on the elliptical fire field model, Zhou Zhiyu et al. used the real-time distance between the transmission tower and the fire field to characterize the failure probability of the transmission tower [8]. However, the above study only focused on the situation of a single wildfire point and did not take into account the actual scenario where transmission lines are often affected by the interaction of multiple fire points during wildfire disasters.

The insulation breakdown failure of transmission lines during the wildfire disaster is the result of a combination of factors. On one hand, the high temperature of the flame significantly reduces the air density. Additionally, the conductivity of the flame itself is much higher than that of the air gap, making the line gap more prone to electron collapse and flow injection [9]. On the other hand, under the influence of thermal air currents, ash particles from vegetation enter the gaps in the power lines, altering the distribution of the electric field and initiating particle discharge. In light of the transmission line failures caused by reduced air gap insulation levels due to mountain fires, Li Peng et al. conducted power frequency breakdown characteristic tests on wire-plate gaps exposed to typical vegetation flames. They analyzed the breakdown mechanism of the gap under flame conditions and developed a flame gap discharge model [10]. Based on the flame combustion model, Zhou Enze et al. [11] modified the withstand voltage of the transmission line's ground insulation and interphase insulation under wildfire disaster conditions [12]. They achieved the calculation of the insulation breakdown probability of the transmission line in the transmission corridor. The above studies focus on traditional AC transmission lines, with limited research on the failure characteristics of HVDC transmission lines during wildfire disasters.

At the same time, the high-voltage HVDC transmission line, with long transmission distances and high voltage levels, plays a crucial role as a hub connecting the new energy power generation base and the load center. In the event of a failure, it can have a significant adverse impact on the systems at both the sending and receiving ends [13–15]. The failure in the HVDC transmission line can result in the blockage of the DC power transmission channel. This can impact the transmission of new energy from the sending end system and lead to various issues, such as power loss in the load and the shedding of the load in the receiving system. The energy imbalance in the power system resulting from a failure in the HVDC line will lead to voltage and frequency fluctuations in the power system. These fluctuations can impact the safe and stable operation of the power system. Therefore, against the backdrop of the escalating wildfire disasters and the growing number of HVDC transmission line constructions and operations, it is crucial to conduct quantitative evaluations and research on HVDC transmission line failure during wildfire disasters to ensure the safe and stable operation of the power system. Starting from the wildfire diffusion model, this paper constructs a failure risk assessment model for HVDC transmission lines under wildfire disasters. The model includes the influence coefficient of the number of fire points, the dynamic factor of failure probability, and the risk factor of the insulation breakdown of HVDC transmission lines. At the same time, the failure risk assessment model is further simplified, and a strong correlation index suitable for the rapid assessment of the failure risk of HVDC transmission lines is proposed. The evaluation effectiveness is verified based on the actual HVDC transmission lines.

3. Methodology and Analysis

3.1. Probability Model of HVDC Line Failure during Wildfire Disasters

Given that various transmission lines are impacted by wildfire disasters to varying extents, the probability of insulation breakdown failure for each transmission line fluctuates in real-time with the progression of the wildfire disasters. Considering the above factors, this paper quantifies the probability of insulation breakdown failure of the kth transmission line during wildfire disasters.

$$P_{line-fire}(k,t) = P_0(k) * P^k_{line}(t) * R_{t-f} \tag{1}$$

where $P_{line-fire}(k,t)$ is the probability of time-varying failure of the kth HVDC transmission line affected by the wildfire disasters and causing insulation breakdown failure, $P_0(k)$ is the influencing factor of the number of different fire points in the influence range of the kth HVDC transmission line, $P^k_{line}(t)$ is used to describe the dynamic factor of the failure probability of the kth HVDC transmission line over time during the wildfire diffusion process [8], and R_{t-f} is the risk factors of the insulation breakdown of HVDC transmission lines during wildfire disasters [11].

3.1.1. Influencing Factor of the Fire Points Number

According to the experience of power grid operation during wildfire disasters, the impact range of a wildfire on a transmission line is limited. According to the actual operation situation, the alarm calculation can be carried out for the transmission line located within the r_0 radius of the impact of the fire points [16]. Therefore, the ratio of the intersection chord length of the circle with the radius of each observed mountain fire in the affected area of the transmission line, with the center denoted as r_0 of the circle, and the intersection chord length of the transmission line and the length of the line is used as the fundamental measure of the transmission line's impact on the number of fire points. This ratio serves as the primary metric for quantifying the influencing factor of the number of fire points. The calculation method is as shown in the following formula.

$$P_0(k) = \frac{\sum_{i=1}^{N(k)} L^k_{i-cicle}}{N(k)L_k} \tag{2}$$

where $N(k)$ is the number of fire points within the influence range of the kth transmission line, L_k is the length of the kth transmission line, and $L^k_{i-cicle}$ is the length of the kth transmission line within the influence range of the concerned wildfire.

3.1.2. Failure Probability Time-Varying Factor

In the absence of wind, the wildfire spreads at a consistent speed in all directions, resulting in circular diffusion. In the presence of wind, the wildfire field takes on an elliptical shape. The longest axis aligns with the direction of maximum wildfire spread. The direction of maximum wildfire spread is determined by the direction of the wind speed [7].

$$\frac{x^2}{\left[1.2e^{1.8v}\varphi\left(\varphi-\sqrt{\varphi^2-1}\right)R_0\Delta t\right]^2}+\frac{y^2}{\left[1.2e^{1.8v}\left(\varphi-\sqrt{\varphi^2-1}\right)R_0\Delta t\right]^2}=1 \tag{3}$$

where v is the wind speed (m/s),R_0 is the initial speed of wildfire spread (m/s),Δt is diffusion time,φ is the shape factor of the elliptical fire field, and (x,y) are, respectively, the horizontal and vertical coordinates of the ellipse centered on the fire point.

Considering that the probability of transmission line failure changes in real time as the distance between the spreading elliptical fire field and the transmission line changes, the weighted sum of the failure probabilities of the transmission towers on both sides of

the transmission line is used to characterize the real-time change in the transmission line failure probability as the elliptical fire field spreads.

$$P_{line}^{k}(t) = \frac{\left\{num_{F}^{k} * P_{tower-F}^{k}(t) + num_{B}^{k} * P_{tower-B}^{k}(t)\right\}}{N} \tag{4}$$

where $P_{tower-F}^{k}(t)$ and $P_{tower-B}^{k}(t)$ are the failure probability dynamic factors of the two adjacent transmission towers in the kth transmission line, respectively [8], num_{F}^{k} and num_{B}^{k} are the fire points numbers within the influence range of the two adjacent transmission towers, respectively, and N is the total number of fire points in the specific area.

3.1.3. HVDC Line Breakdown Risk Factors

When wildfire disasters spread beneath transmission lines, the high-temperature flames and ash produced by burning vegetation significantly reduce the breakdown voltage of the air gap. This reduction may cause phase-to-ground short circuits and phase-to-phase short circuits in the transmission line. Therefore, this paper defines the risk of tripping the overhead transmission lines under wildfire conditions as the greater of the risk between phase-to-ground short circuit between conductors and the ground and the risk of phase-to-phase short circuit between conductors.

The insulation breakdown risk R_{t-f} of HVDC transmission lines during wildfire conditions is defined as the larger value of the line-to-ground breakdown risk R_g and the phase-to-phase breakdown risk R_p [11].

$$R_{t-f} = \max\{R_g, R_p\} \tag{5}$$

$$R_g = \frac{U}{U_g} \tag{6}$$

$$R_p = \frac{2U}{U_p} \tag{7}$$

where U is the voltage level of the HVDC transmission line, and U_g and U_p, respectively, represent the line-to-ground and phase-to-phase air gap withstand voltages during wildfire disasters.

The schematic diagram for calculating the failure probability of HVDC transmission lines during the spread of wildfire disasters is shown in Figure 1.

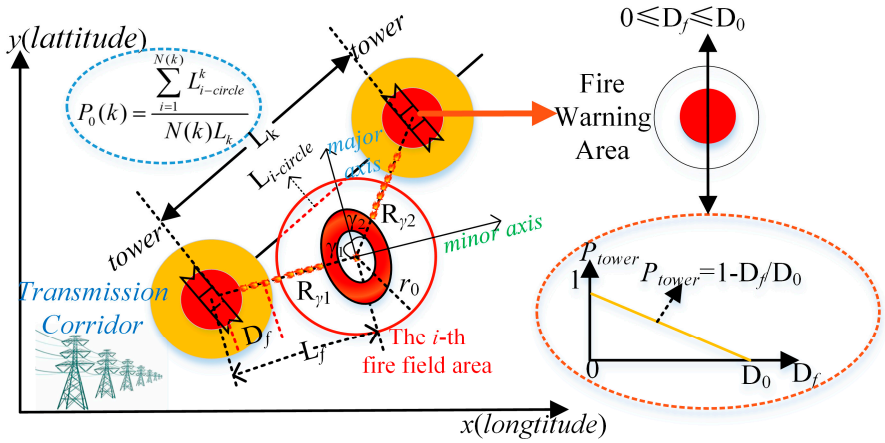

Figure 1. Calculation of the failure probability during wildfire spread.

As shown in Figure 1, γ represents the angle between the initial fire point and the direction of the transmission tower in relation to the major axis of the elliptical fire field, R_γ represents the diffusion velocity in the direction of the γ angle, R_{γ_1} and R_{γ_2} respectively

represent the fire field diffusion velocity in the direction of angles γ_1 and γ_2. D_0 represents the radius of the transmission tower alarm area; r_0 represents the maximum impact radius of the fire field; L_l represents the distance of the transmission line between two adjacent transmission towers; $L_{l,i}$ represents the length of lth transmission lines in the ith fire-affected area. L_f represents the distance between the fire point and the transmission tower at the initial moment; $D_f = L_f - R_\gamma t$ represents the real-time distance between the spreading field boundary of wildfire and the transmission tower at t moment.

For long-distance transmission lines composed of multiple transmission branches, the probability of failure of a long-distance transmission line composed of n transmission branches during wildfire disasters can be calculated using the probability algorithm.

$$P^i_{trans-fire} = 1 - \prod_{k=1}^{n} \left[1 - P^i_{trans-fire}(k)\right] \tag{8}$$

where $P^i_{trans-fire}$ is the failure probability of the ith transmission line during wildfire disasters, $P^i_{trans-fire}(k)$ is the failure probability of the kth transmission branch in the ith long-distance transmission line during wildfire disasters, and n is the number of branches included.

3.2. Constructing Methodology of the Simplified Evaluation Index

For the actual HVDC transmission line, it contains a large number of transmission branches. When a large-scale wildfire disaster spreads, it is challenging to calculate the failure probability of HVDC transmission lines using the formula above to meet the rapid response requirements of the power system. Therefore, it is necessary to propose simplified evaluation indicators to achieve a rapid and accurate evaluation of transmission line failure probability during wildfire disasters.

Given that the impact range of wildfire disasters is significantly smaller than the geographical distance covered by HVDC transmission lines, the number of branches of HVDC transmission lines affected by wildfire disasters is limited. Therefore, the failure probability of the kth transmission branch in the ith long-distance transmission line during wildfire disaster is approximately zero. At the same time, considering that when $x_k \to 0\,(k = 1 \ldots n)$, the binomial expansion can be obtained by ignoring higher-order terms more than once.

$$1 - \prod_{k=1}^{n} (1 - x_k) = \sum_{k=1}^{n} x_k + o(\sum_{k=1}^{n} x_k) \tag{9}$$

where $o(\sum_{k=1}^{n} x_k)$ is the higher-order peano infinitesimals.

Therefore, equation (8) can be approximated as follows:

$$P^i_{trans-fire} = \sum_{k=1}^{n} P^i_{trans-fire}(k) \tag{10}$$

Therefore, the evaluation index can be constructed as follows:

$$E_S = \frac{N_S}{N} \tag{11}$$

where N_S is the total number of fire points in the buffer zone of long-distance HVDC transmission lines, and E_S is the constructed evaluation index.

3.3. ArcGIS Processing Module

It can be seen from the line failure probability calculation model under wildfire conditions proposed above that a major difficulty in the implementation of this model lies in the rapid and accurate calculation of the number of fire points in the circular buffer zone of all transmission towers. With the recent advancements in satellite remote sensing

technology, such as the MOD14 product (wildfire/temperature anomaly detection) in the Modis series developed by NASA and the Fengyun-3 meteorological satellite, real-time monitoring of forest fires every 5 min has become possible [17–19]. The fire point data obtained by satellites consist of historical longitude and latitude coordinates of fire points in a specific year and month. Efficiently utilizing existing satellite data to count the number of fire points within specific buffer zones is an urgent issue that requires resolution. It is also urgent to address the issue of obtaining accurate mountain fire point data. Probability calculations and essential operations are crucial for rigorously assessing risk. Therefore, this paper proposed an algorithm for calculating the number of fire points in the buffer zone of automated batch transmission towers using ArcGIS. It also included practical development and processing on the ArcGIS platform [20]. The automated batch retrieval algorithm process developed based on the ArcGIS platform is shown in Figure 2.

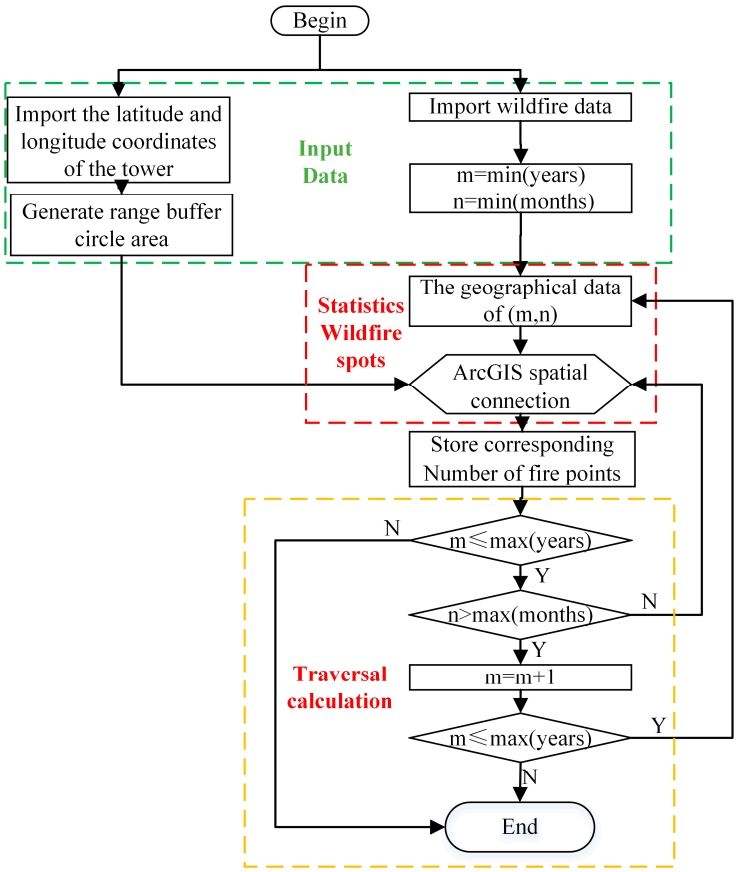

Figure 2. ArcGIS fire point statistical processing flow chart.

To effectively utilize satellite-acquired wildfire hotspots data and promptly calculate the number of wildfire hotspots within the buffer zones of transmission lines, an automated toolbox for batch statistics of wildfire hotspot counts within the buffer zones of transmission towers was developed using the ArcGIS geographic information processing platform. The automated batch-processing workflow is illustrated in Algorithm 1.

Algorithm 1 Batch rapid fire point counting process in the buffer zone

Process: Automated batch statistics of the number of fire points within the impact area of transmission towers.
Input: Latitude and longitude of transmission towers
Longitude and latitude data of the wildfire

(1) Use the ArcGIS buffer generation module to generate
a circular influence area of the transmission towers.

(2) for i = 1:M(The maximum value of the years)
for j = 1:N(The maximum value of the months) do
Utilizing the ArcGIS Spatial Join module to perform statistical analysis on all fire points within the buffer zones of transmission towers for the specified date.
end for
end for

Output: The number of fire points in the transmission towers buffer zone.

4. Case Study Results

4.1. Introduction to the Calculation System

In order to demonstrate the practicality of the model algorithm, this article selected six HVDC transmission channels in the Sichuan Province, China as calculation examples [21–24]. Their basic information is shown in the Table 1.

Table 1. The information about HVDC transmission lines.

Send node	Receiver	Length	Voltage
Baihetan	Zhejiang	2121 (km)	800 kV
Baihetan	Jiangsu	2080 (km)	800 kV
Deyang	Baoji	534 (km)	500 kV
Fulong	Fengxian	1907 (km)	800 kV
Shuanglong	Jinhua	1680 (km)	800 kV
Yazhong	Boyanghu	1696 (km)	800 kV

The source of the wildfire coordinates and longitude and latitude data in this example was MODIS data [25]. Figure 3 illustrates the distribution of wildfire spots by year in the buffer zones of six HVDC transmission lines from 2001 to 2022.

As can be seen from the Figure 3, the number of wildfire spots in the buffer zone varied significantly due to differences in geographical environment, line length, and other parameters of different HVDC transmission lines. For the Debao HVDC transmission line, the line length was short, and the number of fire points in the buffer zone was small. The peak number of fire points was only about 300. Since 2016, it has had zero fire incidents for many years. The failure probability was zero, even when affected by wildfires. Disaster impacts cannot be ignored. For the Yazhong HVDC transmission line, the line length was extensive, the geographical coverage was vast, and there was a large number of fire points in the buffer zone. In 2010, it reached a historical peak of about 2000. Since 2015, the number of fire points has remained relatively stable at about 500 wildfire spots. The impact of wildfire disasters on the Yazhong HVDC transmission line cannot be ignored. For the four HVDC transmission lines—Xizhe, Baihetan-Jiangsu, Baihetan-Zhejiang, and Fufeng—there was a noticeable trend of frequent fire occurrences in the buffer zones adjacent to these lines. The peak number of fire incidents occurred around 2013. The maximum number was around 4000. Since 2015, the number of fire incidents has been steadily increasing. The impact of wildfire disasters on these HVDC transmission lines has become increasingly serious.

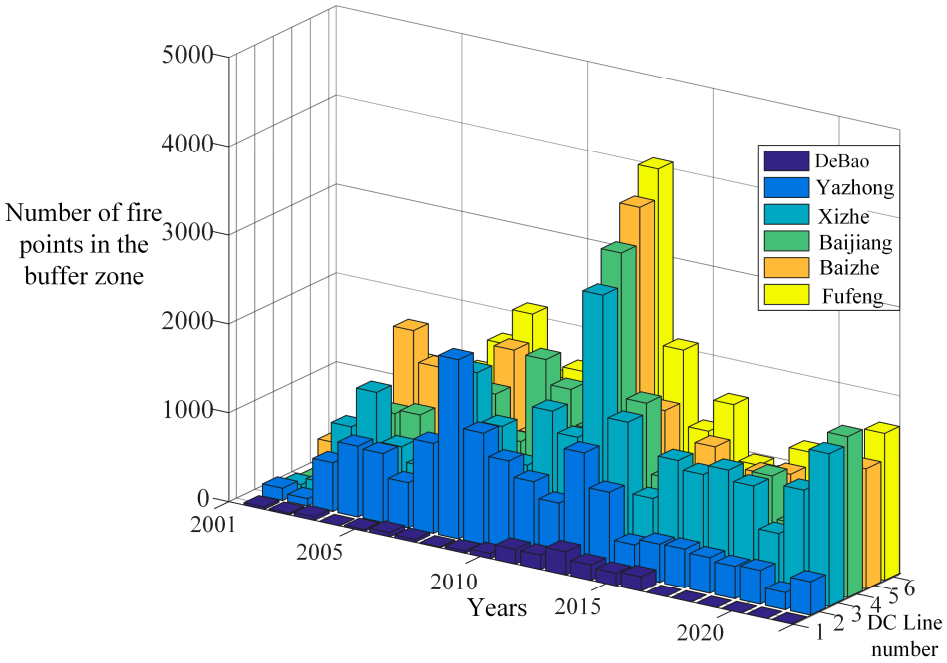

Figure 3. Distribution of wildfire point numbers in the line buffer zone.

4.2. Analysis of Failure Probability Calculation Results

For the Baihetan-Zhejiang 800 kV HVDC transmission line, it can be observed from Figure 4 that the HVDC transmission line is significantly impacted by wildfire disasters, with a probability of failure each month. Among them, the probability of failure is higher in January, February, March, November, and December. Therefore, the high-incidence periods for this HVDC transmission line are early winter and early spring. The highest failure probability calculated according to the model is about 0.09 and occurs in January. In these months, the focus should be on preventing wildfire disasters.

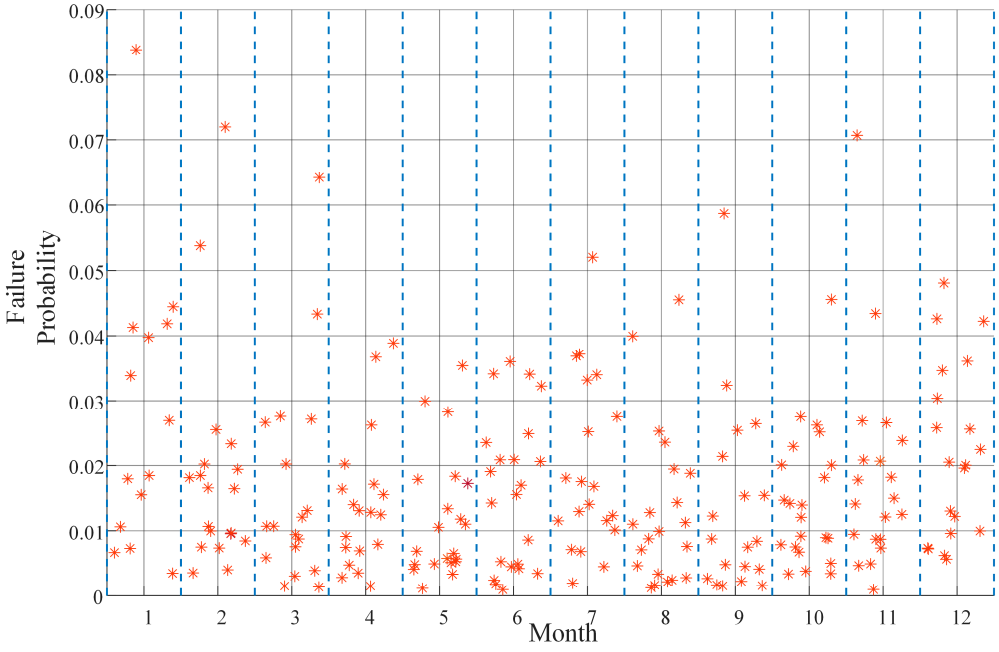

Figure 4. Baihetan-Zhejiang HVDC transmission line failure probability by month.

As for the Baihetan-Jiangsu 800 kV HVDC transmission line, it can be observed from Figure 5 that this HVDC transmission line is also significantly impacted by wildfire

disasters, with a certain probability of failure each month. Among them, the failure probability is higher in June, July, September, October, and December. Therefore, the high-incidence periods for this HVDC transmission line are summer and early winter. The highest failure probability calculated according to the model is about 0.06, which occurs in October and December. During these months, special attention should be paid to preventing wildfire disasters.

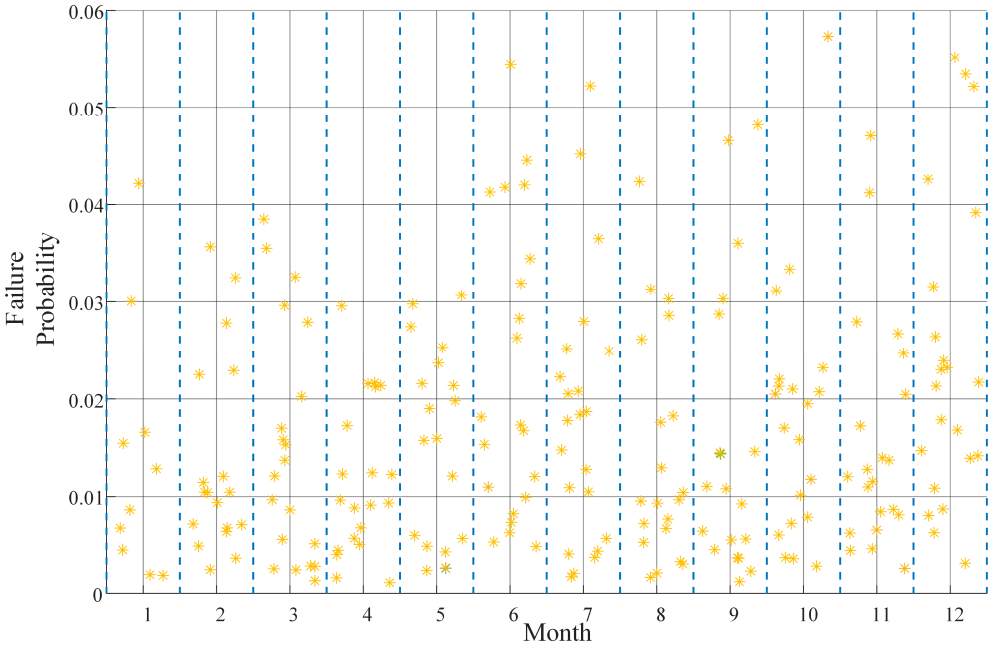

Figure 5. Baihetan-Jiangsu HVDC transmission line failure probability by month.

For the Deyang-Baoji 500 kV HVDC transmission line, it can be observed from Figure 6 that the line is less susceptible to wildfire disasters. Although there is a risk of failure, the probability distribution of failure is relatively low. This means that the HVDC transmission line is mostly reliable during most periods of time. Transmission lines operate stably and without failure. Among them, the probability of failure is higher in June, July, and August. Therefore, the period of high failure occurrence for this HVDC transmission line is summer. At the same time, the probability of failure in October, November, and December is 0, indicating no risk of wildfire disaster failure in HVDC transmission lines during the early winter months. The highest failure probability calculated according to the model is about 0.06, which occurs in August. During these months, it is crucial to focus on preventing wildfire disasters.

For the Fulong-Fengxian 800 kV HVDC transmission line, it can be observed from Figure 7 that this HVDC transmission line is significantly impacted by wildfire disasters. The failure probability is notably high and concentrated each month. Among them, the probability of failure is higher in March, April, May, June, and September. This means that the periods of HVDC transmission line failures are in the spring and summer. The highest failure probability calculated according to the model is about 0.15 in April. During these months, the focus should be on preventing wildfire disasters.

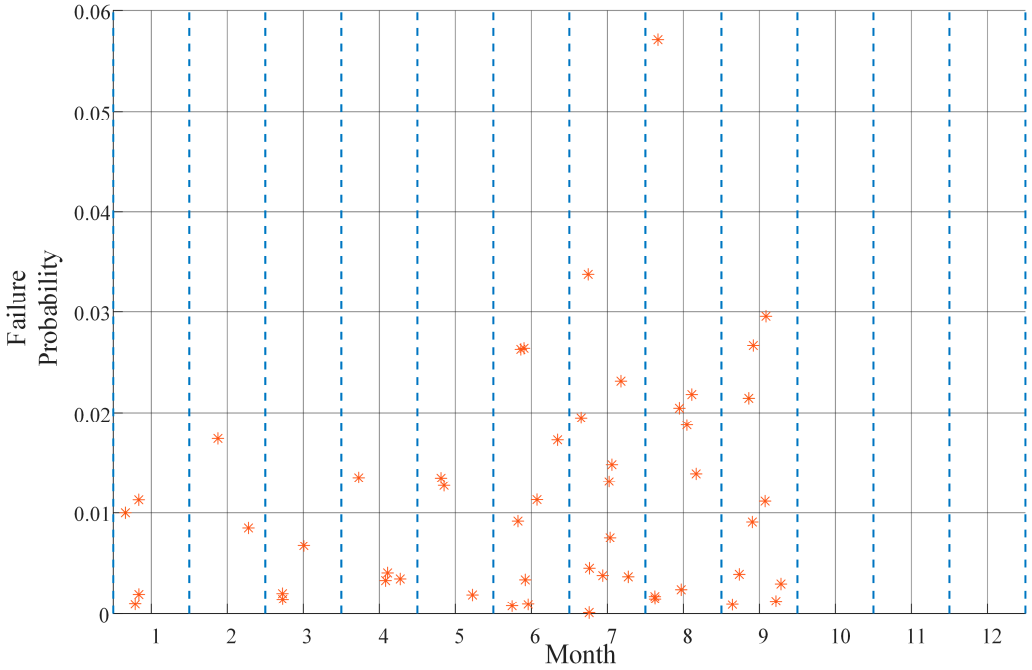

Figure 6. Deyang-Baoji HVDC transmission line failure probability by month.

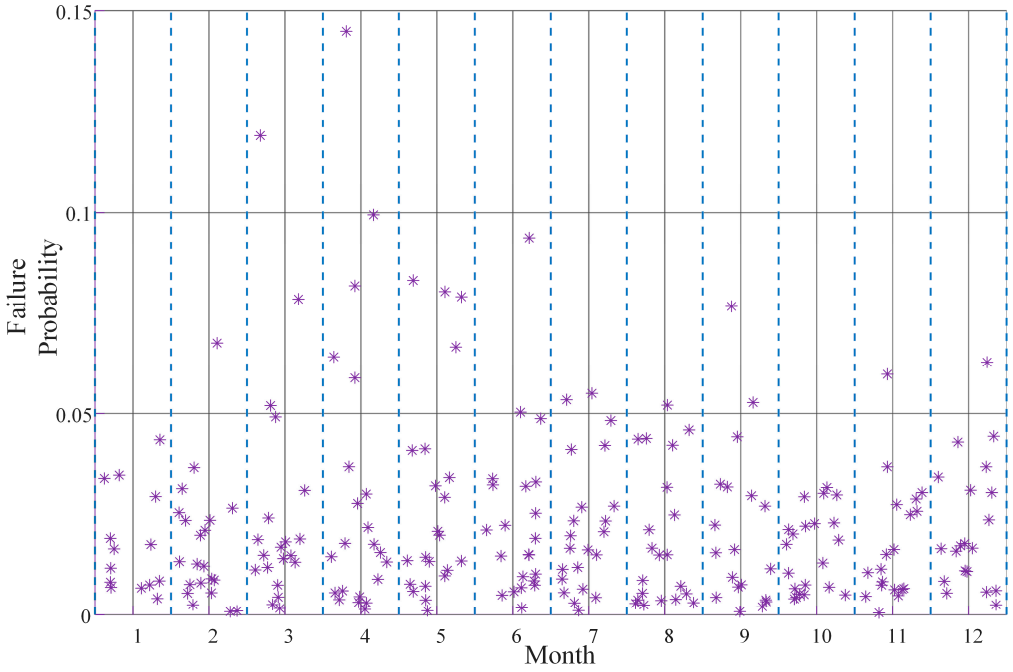

Figure 7. Fulong-Fengxian HVDC transmission line failure probability by month.

For the Shuangyong-Jinhua 800 kV HVDC transmission line, it can be observed from Figure 8 that the line is significantly impacted by wildfire disasters, leading to a relatively high probability of HVDC failure each month. Among them, the probability of failure is higher in May, July, August, October, and December. Therefore, the high-incidence periods for this HVDC transmission line are summer and early winter. The highest failure probability calculated according to the model is about 0.1, which occurs in December. During these months, it is crucial to focus on preventing wildfire disasters.

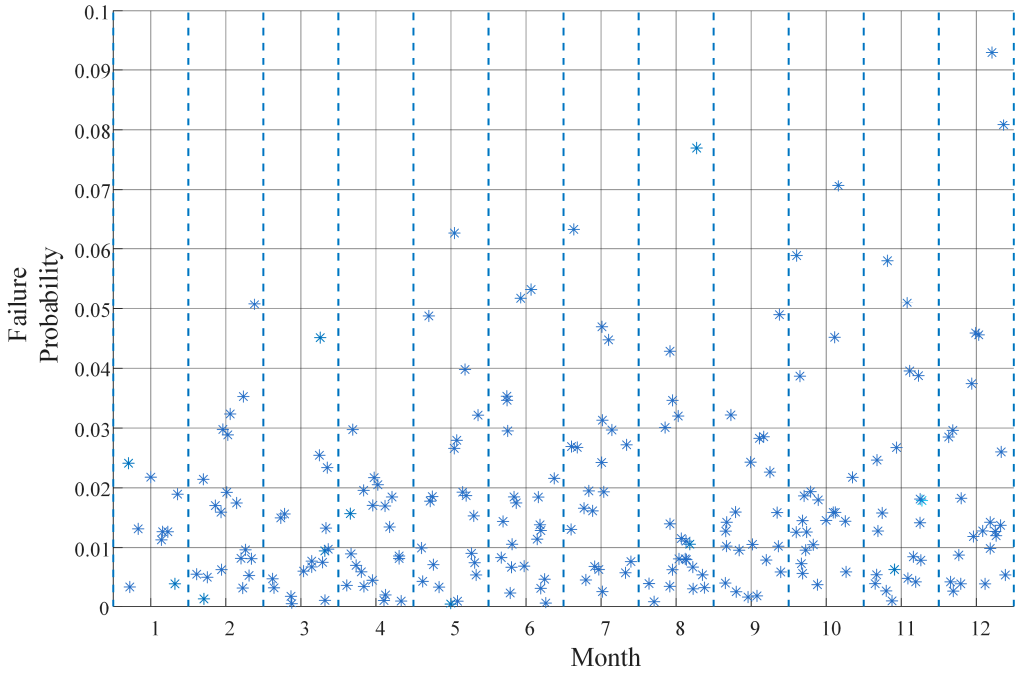

Figure 8. Shuanglong-Jinhua HVDC transmission line failure probability by month.

For the 800 kV Yazhong HVDC transmission line, as shown in Figure 9, it is evident that the line is less susceptible to wildfire disasters, resulting in a low failure probability throughout each month. Among them, the probability of failure is higher in May, July, August, and November. Therefore, the high-incidence periods for this HVDC transmission line are summer and early winter. The highest failure probability calculated according to the model is about 0.06, which occurs in May. During these months, it is crucial to focus on preventing wildfire disasters.

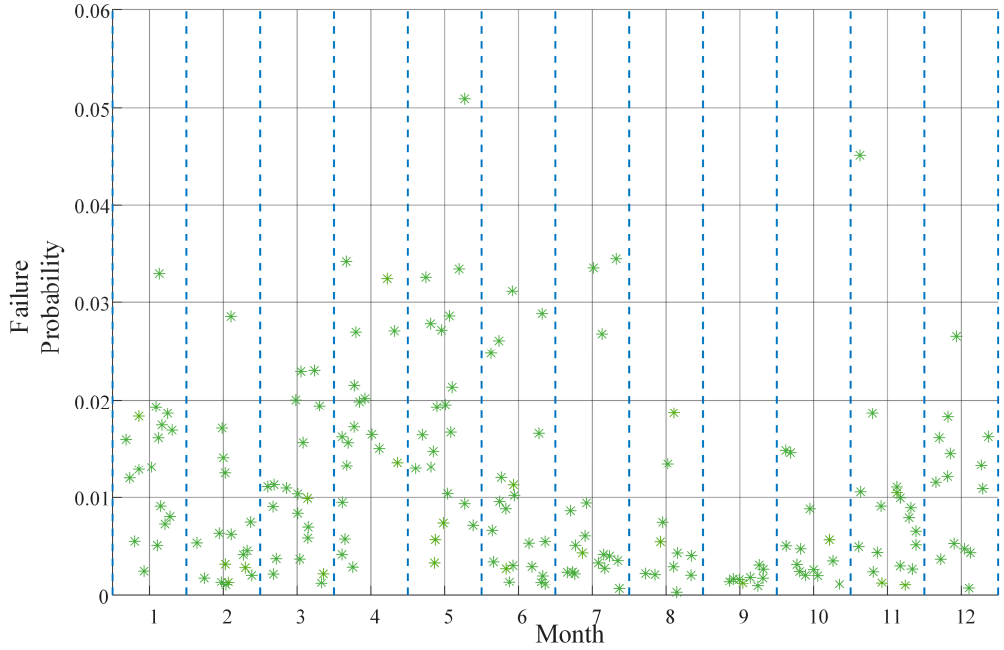

Figure 9. YaZhong HVDC transmission line failure probability by month.

4.3. Evaluation Indicator Effectiveness Analysis

The effectiveness of the evaluation index E_S proposed in this article was verified using linear regression analysis [26–28]. The evaluation index E_S was plotted on the horizontal axis, while the failure probability of HVDC transmission lines during wildfire disasters was plotted on the vertical axis. The data scatter points and regression lines of each HVDC transmission line are shown in Figure 10.

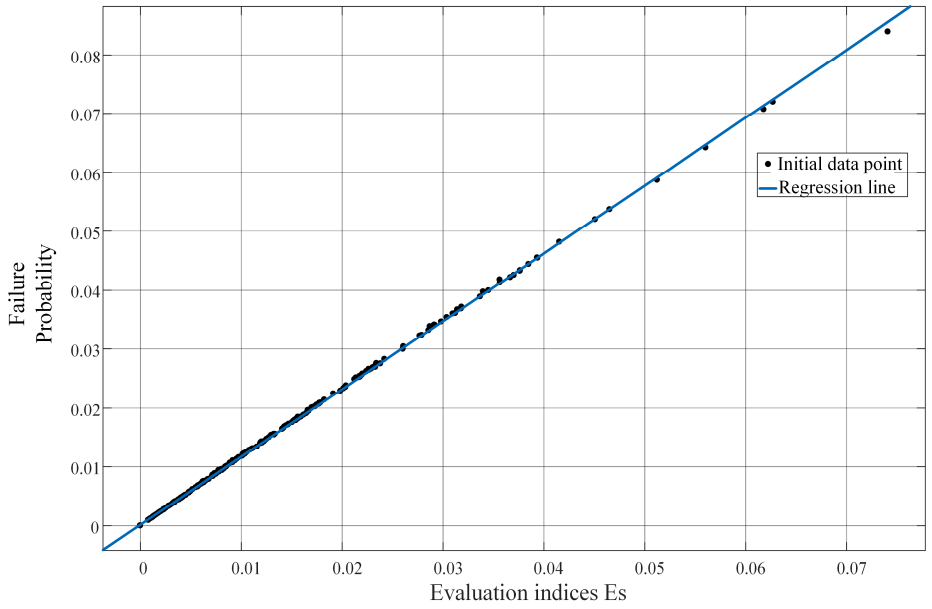

(**a**)

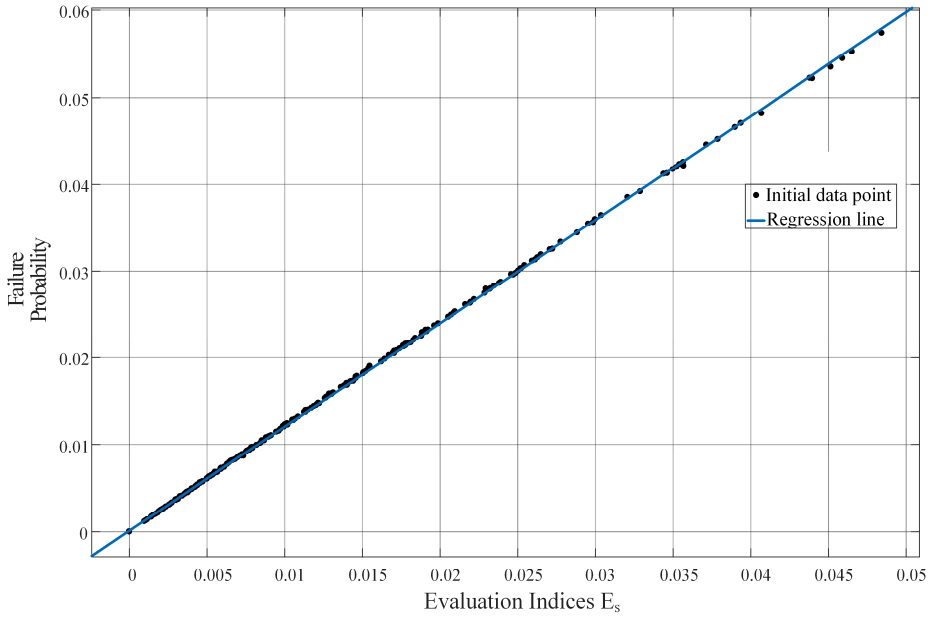

(**b**)

Figure 10. *Cont.*

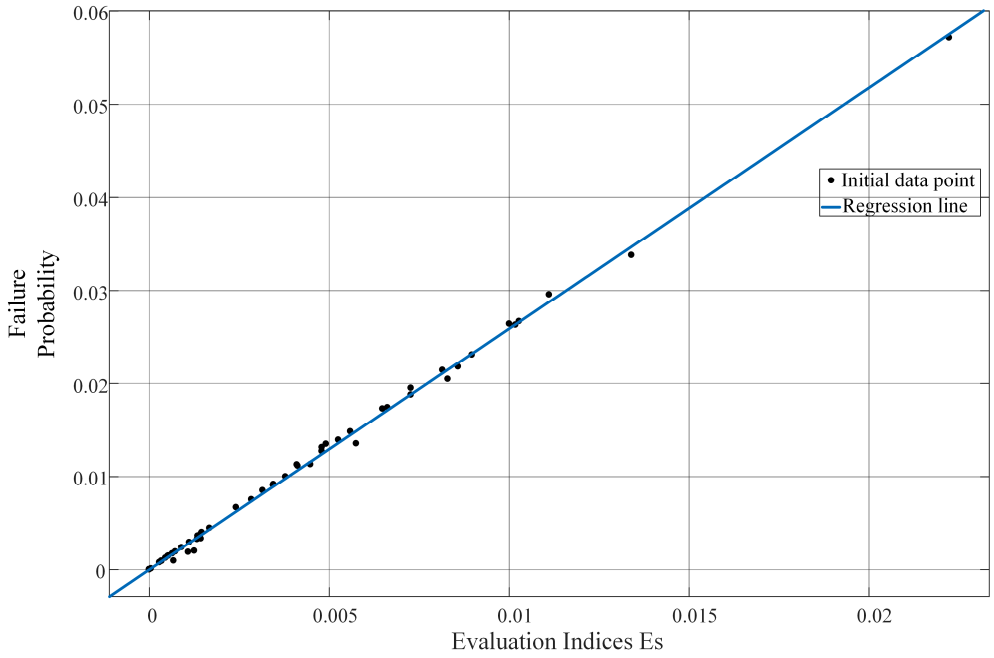

(**c**)

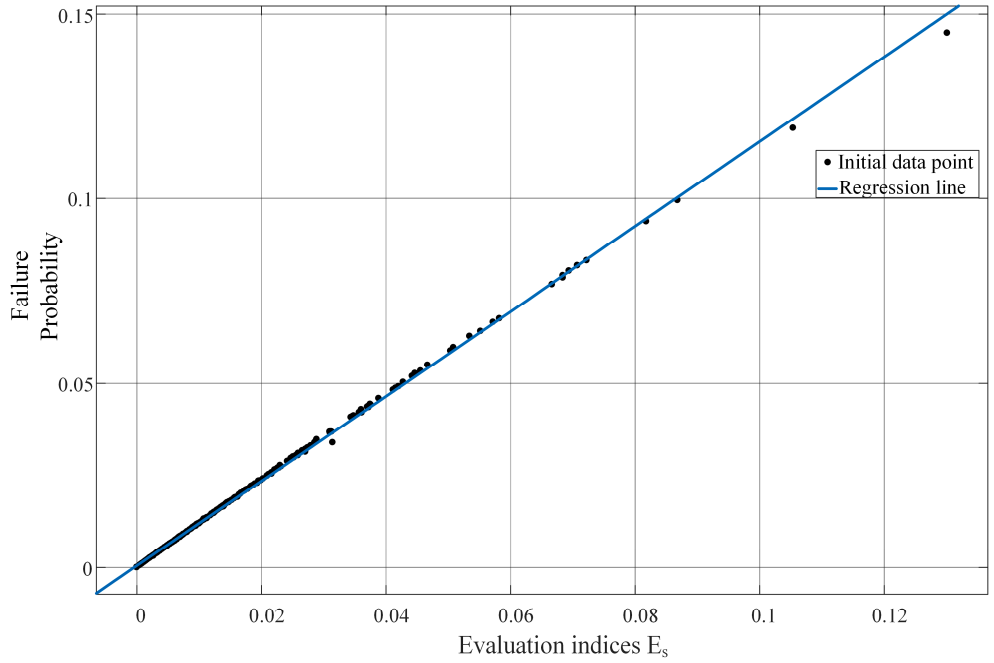

(**d**)

Figure 10. *Cont*.

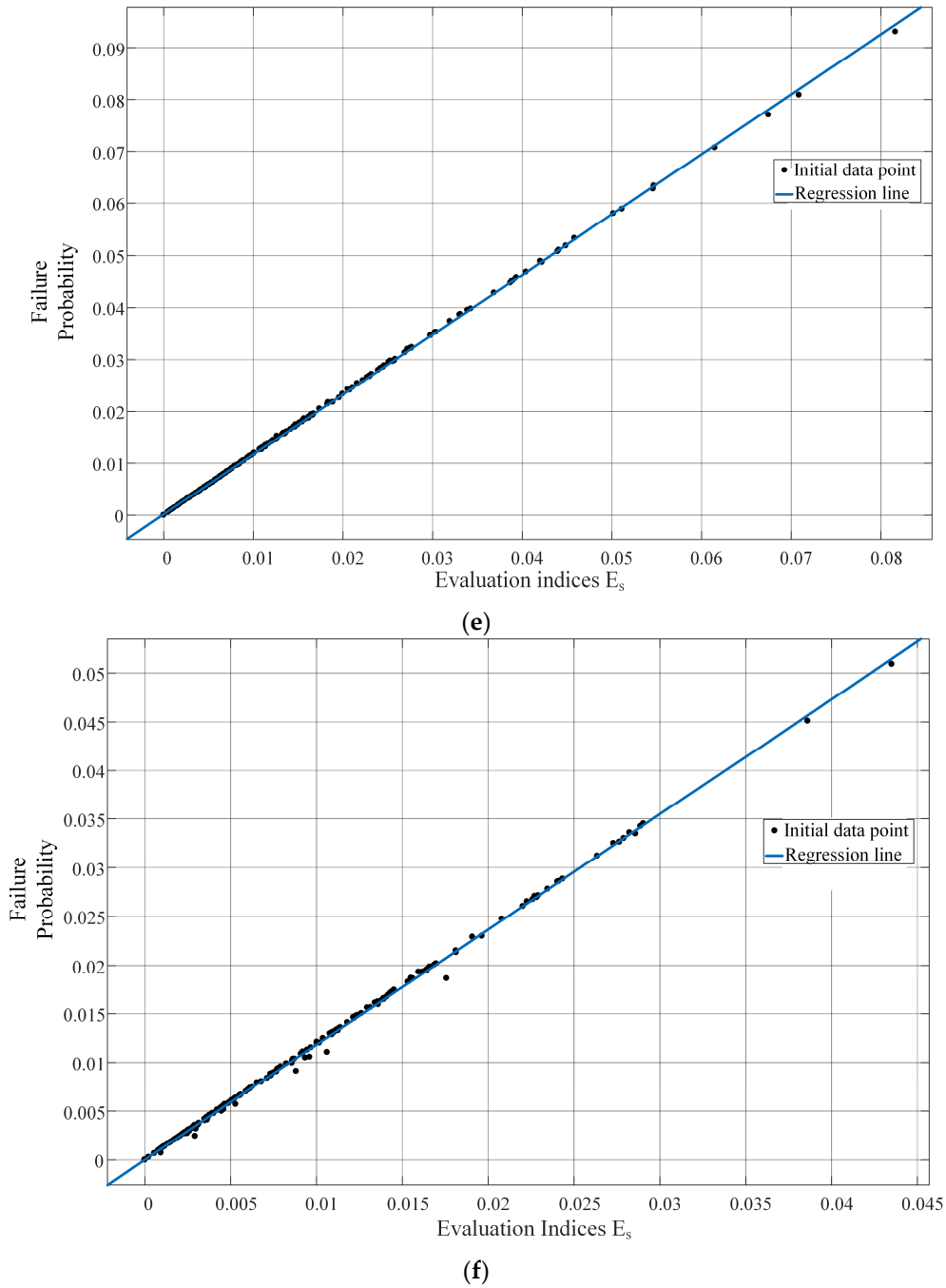

Figure 10. Regression analysis chart of each HVDC transmission line. (**a**) Baihetan-Zhejiang transmission line; (**b**) Baiehtan-Jiangsu transmission line; (**c**) Deyang-Baoji transmission line; (**d**) Fulong-Fengxian transmission line; (**e**) Shuanglong-Jinhua transmission line; and (**f**) Yazhong HVDC transmission line.

It can be seen from Figure 10 that the evaluation indicators and failure probabilities of each HVDC transmission line had a strong linear correlation. The corresponding linear correlation index (R^2) and residual sum of squares (SSE) are shown in Table 2.

As can be seen from Table 1, the correlation index (R^2) was above 0.999, indicating that the two variables above had a strong linear relationship. The residual sum of squares (SSE) was in the order of 10^{-5}, and the smallest one was 5.2581×10^{-6}. This shows that the proposed evaluation index can be used to effectively evaluate the failure probabilities of HVDC transmission lines during wildfire disasters.

Table 2. Relationship indicators of each HVDC transmission line.

HVDC Line	R^2	SSE
Baihetan-Zhejiang	0.9998	1.0328×10^{-5}
Baihetan-Jiangsu	0.9999	5.2581×10^{-6}
Deyang-Baoji	0.9990	1.1822×10^{-5}
Fulong-Fengxian	0.9993	8.0698×10^{-5}
Shuanglong-Jinhua	0.9998	1.1345×10^{-5}
Yazhong	0.9994	1.4995×10^{-5}

5. Discussion

In this paper, we conducted a study on the failure probability calculation methodology of HVDC transmission lines during wildfire disasters for accurately and rapidly assessing the failure risk of HVDC transmission lines. The calculation model considering the multiple influences of wildfire spots numbers, diffusing wildfire characteristics, and parameters of HVDC transmission line was established, and it was used to assess the actual HVDC transmission line failure risks on different dates. The results indicated that the different transmission lines had different failure probability characteristics, which behaved based on the distribution of the time dimension and the value of probability. By analyzing the calculation results based on the probability model, we can provide useful information for power grids to reduce the economic loss caused by wildfire disasters. Meanwhile, we proposed a simplified evaluation index and built an ArcGIS module to rapidly assess the transmission line failure risk. The effectiveness of the proposed methodology was validated by regression analyzing.

However, the proposed model also has some limitations and challenges in actual application. Firstly, the effectiveness of the probability model needs to be verified with actual failure probability data, but obtaining the actual failure probability data is difficult and unrealistic. This was obvious when applying imitation to this model. Secondly, the cases studied in this paper are limited, and the model should be assessed by calculating more actual transmission lines. Our future work will concentrate on the further refinement of the calculation model.

6. Conclusions

This article conducted significant research on calculating the failure probabilities of HVDC transmission lines during wildfire disasters. Taking a number of actual hydro-power HVDC transmission lines in the Sichuan Province, China as examples, the novelty and contribution of this work are as follows:

(1) The proposed method for calculating failure probability comprehensively considers various factors influencing wildfire disasters on HVDC transmission lines. It can effectively evaluate the impact of wildfire disasters on HVDC transmission lines. In previous studies about calculating the transmission line failure probability during wildfire disasters, as shown in references [14,15], the multiple influences of the various wildfire spots in reference [15] and the influence of different transmission line characteristics, such as voltage level [14], are not considered. This paper establishes a calculating model considering the various wildfire spots, the diffusion of wildfire disasters, and the transmission line characteristics.

(2) For actual HVDC transmission lines, the failure risk assessment index proposed in this article can accurately evaluate the failure risk of HVDC transmission lines during wildfire disasters and has practical application value. The simplified evaluation index is proposed to accurately assess the failure risk of transmission lines during wildfire disasters, and its accuracy is verified by regression analysis. By using this simplified evaluation index in the large-scale transmission grid, the calculation time can be reduced, and the computational efficiency can be improved.

(3) This paper proposes a processing method of various wildfire spots and develops an automatic processing toolbox based on the ArcGIS. This allows us to obtain the wildfire spots numbers in the buffer zone accurately and rapidly and provides the critical information to calculate the simplified evaluation index.

Meanwhile, the discussion of limitations and potential future work are as follows:

(1) The computing accuracy of the simplified index and the proposed calculating modelshould be validated by comparing them with the real failure data of transmission lines.

(2) The potential future work will concentrate on the validation of the proposed calculating model accuracy and expand this model and its simplification method to calculate the transmission line failure during other extreme disasters, such as typhoons and earthquakes.

Author Contributions: Investigation, B.Z.; methodology, B.Z.; validation, B.Z. and Y.X.; writing—original draft preparation, B.Z.; writing—review and editing, B.Z. and X.S.; supervision, W.W. All authors have read and agreed to the published version of the manuscript.

Funding: This work was supported by the State Grid Sichuan Electric Power Research Institute Science and Technology Project under Grant 52199723001F (Research on Power Grid Resilience Assessment and Multi-resource Coordinated Resilience Enhancement Technology under Unconventional Conditions).

Data Availability Statement: The raw data supporting the conclusions of this article will be made available by the authors upon request.

Conflicts of Interest: All authors were employed by The STATE GRID COOPRATION OF CHINA(SGCC).

References

1. Liang, Y.; Zhou, L.; Chen, J.; Huang, Y.; Wei, R.; Zhou, E. Monitoring and Risk Assessment of Wildfires in the Corridors of High-Voltage Transmission Lines. *IEEE Access* **2020**, *8*, 170057–170069. [CrossRef]
2. Erickson, E.; Slobodin, R.; Poshtan, M.; Taufik, T.; Callenes, J. Using Power Infrastructures for Wildfire Detection in California. In Proceedings of the 2020 IEEE Power & Energy Society Innovative Smart Grid Technologies Conference (ISGT), Washington, DC, USA, 17–20 February 2020; pp. 1–5.
3. Cai, S.K.; Li, S.; Wang, J.Y.; Meng, G.J.; Cui, J.J. Research on monitoring and early warning technology of transmission line wildfire. *Manuf. Autom.* **2023**, *45*, 31–35.
4. Wu, T.; Hu, Y.; Ruan, J.-J.; Liu, K.; Liu, T.; Chen, C. Air gap breakdown mechanism of model AC transmission line under forest fires. *High Volt. Technol.* **2011**, *37*, 1115–1122.
5. Yang, C.L.; Ning, X.; Xu, H.K.; Chen, T.X.; Zeng, C.X.; Yang, S. Overview of wildfire monitoring and early warning for power grid demand. *Power Syst. Technol.* **2023**, *47*, 4765–4777.
6. Li, J.; Cao, Y.X.; Zhu, J.; Luo, D.H. Research on real-time radar monitoring technology and its application to forest fire around transmission line. *Sichuan Electr. Power Technol.* **2021**, *44*, 53–57.
7. Anderson, D.H.; Catchpole, E.A.; De Mestre, N.J.; Parkes, T. Modelling the spread of grass fires. *ANZIAM J.* **1982**, *23*, 451–466. [CrossRef]
8. Zhou, Z.; Ai, X.; Lu, J.; Liu, X. A Real-time Analysis Approach and Its Application of Transmission Line Trip Risk due to Wildfire Disaster. *Proc. Chin. Soc. Electr. Eng.* **2017**, *37*, 5321–5330.
9. Pu, Z.; Xiong, Y.; Wu, T.; Lu, Z.; Fang, C. Simulation Analysis on Influence of Combustion Particles on the Gap Electric Field under DC Voltage. In Proceedings of the 2018 IEEE International Conference on High Voltage Engineering and Application (ICHVE), Athens, Greece, 10–13 September 2018; pp. 1–4.
10. Li, P.; Huang, D.; Ruan, J.; Wei, H.; Qin, Z.; Long, M.; Wu, T. Influence of forest fire particles on the breakdown characteristics of air gap. *IEEE Trans. Dielectr. Electr. Insul.* **2016**, *23*, 1974–1984. [CrossRef]
11. Zhou, E.; Yang, F.; Zhang, L. Wildfire Early Warning of Power Grid Failure Rate Based on Modified Ellipse Model. In Proceedings of the 2019 IEEE 3rd Conference on Energy Internet and Energy System Integration (EI2), Changsha, China, 8–10 November 2019; pp. 815–819.
12. Fonseca, J.R.; Tan, A.L.; Silva, R.P.; Monassi, V.; Assuncao, L.A.R.; Junqueira, W.S.; Melo, M.O.C. Effects of agricultural fires on the performance of overhead transmission lines. *IEEE Trans. Power Deliv.* **1990**, *5*, 687–694. [CrossRef]
13. Muniappan, M. A comprehensive review of DC fault protection methods in HVDC transmission systems. *Prot. Control Mod. Power Syst.* **2021**, *6*, 1. [CrossRef]

14. Su, C.; Yin, C.; Li, F.; Han, L. A Novel Recovery Strategy to Suppress Subsequent Commutation Failure in an LCC-Based HVDC. *Prot. Control Mod. Power Syst.* **2024**, *9*, 38–51. [CrossRef]
15. Yao, Z.; Zhang, Q.; Chen, P.; Zhao, Q. Research on Fault Diagnosis for MMC-HVDC Systems. *Prot. Control Mod. Power Syst.* **2016**, *1*, 8. [CrossRef]
16. Lu, J.; Guo, J.; Jian, Z.; Xu, X. Optimal Allocation of Fire Extinguishing Equipment for a Power Grid Under Widespread Fire Disasters. *IEEE Access* **2018**, *6*, 6382–6389. [CrossRef]
17. Zhou, W.; Chen, W.; Zhou, E.; Huang, Y.; Wei, R.; Zhou, Y. Prediction of Wildfire-induced Trips of Overhead Transmission Line based on data mining. In Proceedings of the 2020 IEEE International Conference on High Voltage Engineering and Application (ICHVE), Beijing, China, 6–10 September 2020; pp. 1–4.
18. Kaufman, Y.J.; Justice, C.; Flynn, L.; Kendall, J.; Giglio, L.; Prins, E.; Setzer, A. Monitoring global fires from EOS-MODIS. *J. Geophys. Res.* **1998**, *103*, 215–239. [CrossRef]
19. Qin, X.L.; Yi, H.R. A method to identify forest fire based on MODIS data. *Fire Saf. Sci.* **2004**, *2*, 83–89.
20. Yankovich, E.P.; Baranovskiy, N.V.; Yankovich, K.S. ArcGIS for assessment and display of the probability of forest fire danger. In Proceedings of the 2014 9th International Forum on Strategic Technology (IFOST), Cox's Bazar, Bangladesh, 21–23 October 2014; pp. 222–225.
21. Shao, Z.; Lu, J.; Lu, Y.; Zou, Q.; Liu, C. Research and application of the control and protection strategy for the ±500kV Xiluodu-Guangdong double bipole HVDC project. In Proceedings of the 2011 4th International Conference on Electric Utility Deregulation and Restructuring and Power Technologies (DRPT), Weihai, China, 6–9 July 2011; pp. 88–93.
22. Rao, H.; Zhang, D.; Zhao, X.; Guo, Q. Practice and Analyses of UHVDC Power Transmission. *High Volt. Eng.* **2015**, *41*, 2481–2488.
23. Li, L. Technical characteristics and engineering application of UHV DC transmission. *Autom. Electr. Power Syst.* **2005**, *2005*, 5–6.
24. Chen, M.; Rao, H.; Li, L.; Guo, J.; Li, X.; Xu, S. Analysis on the Main Wiring of Nan'ao VSC-HVDC Tranmission System. *South. Power Syst. Technol.* **2012**, *6*, 1–5.
25. Giglio, L.; Chroeder, W.S. A global feasibility assessment of the bi-spectral fire temperature and area retrieval using MODIS data. *Remote Sens. Environ.* **2014**, *152*, 166–173. [CrossRef]
26. Jarman, K.H. *The Art of Data Analysis: How to Answer Almost Any Question Using Basic Statistics*; Wiley Blackwell: Hoboken, NJ, USA, 2013; pp. 1–179. [CrossRef]
27. Guo, P.-X.; Datta-Gupta, A.; Valko, P. Optimal Transformations for Multiple Regression: Application to Permeability Estimation From Well Logs. *SPE Form. Eval.* **1997**, *12*, 85–93.
28. Hosmer, D.W.; Lemeshow, S.; Sturdivant, R.X. *Applied Logistic Regression*, 3rd ed.; Wiley: Hoboken, NJ, USA, 2013; pp. 1–510. [CrossRef]

Disclaimer/Publisher's Note: The statements, opinions and data contained in all publications are solely those of the individual author(s) and contributor(s) and not of MDPI and/or the editor(s). MDPI and/or the editor(s) disclaim responsibility for any injury to people or property resulting from any ideas, methods, instructions or products referred to in the content.